RSC Advances

PAPER

View Article Online
View Journal | View Issue

Cite this: *RSC Adv.*, 2019, **9**, 9079

Comparison of electrochemical performance of $LiNi_{1-x}Co_xO_2$ cathode materials synthesized from coated $(1-x)Ni(OH)_2@xCo(OH)_2$ and doped $Ni_{1-x}Co_x(OH)_2$ precursors†

Lei Tang,[a] Gang Li,[b] Peng Xiao,[a] Xu Chen[a] and Wensheng Yang*[a]

Received 10th December 2018
Accepted 11th March 2019

DOI: 10.1039/c8ra10116g

rsc.li/rsc-advances

$LiNi_{1-x}Co_xO_2$ cathode materials were successfully synthesized from coated $(1-x)Ni(OH)_2@xCo(OH)_2$ and doped $Ni_{1-x}Co_x(OH)_2$ precursors, and the effects of the Co site and content in the precursor and final cathode material on the structure, morphology, and electrochemical performance of the cathodes were investigated using X-ray diffraction, scanning electron microscopy, and charge–discharge tests. The electrochemical performance of the materials prepared from the coated precursor was generally better than that of the materials prepared from the doped precursor. However, with increasing Co content, the performance difference gradually decreased. Among the as-prepared samples, the sample coated with 12 mol% Co delivered an excellent reversible capacity of 213.8 mA h g^{-1} at 0.1C and the highest capacity retention of 88.5% after 100 cycles at 0.2C in the voltage range of 2.75–4.3 V. High-performance $LiNi_{1-x}Co_xO_2$ materials were successfully synthesized, and our findings clearly reveal the differences in the electrochemical properties of the materials prepared from the two different precursors with increasing Co content, thereby providing a valuable reference for the synthesis of high-performance Ni-rich layered cathode materials for Li-ion batteries.

1. Introduction

Li-ion batteries (LIBs) have been widely used for various applications ranging from portable electronic devices to electric vehicles (EVs) because of their excellent power and energy densities.[1–3] Recently, there has been increased demand for longer standby times for smartphones and longer driving ranges for EVs, both of which require LIBs with higher energy densities.[4–6] To resolve these issues, Ni-rich binary and ternary layered $LiNi_{1-x}M_xO_2$ ($1-x > 0.6$) materials have been developed by doping other metals M (M = one or two metals among Co, Mn, Mg, Al, Ti, Zr, *etc.*) into the host structure of $LiNiO_2$ because of their high reversible capacity (>190 mA h g^{-1}).[7–9] The synthesis of Ni-rich layered materials is much less difficult than that of $LiNiO_2$. In addition, the structural stability upon cycling can also be improved,[10] which is mainly attributed to the reduction of Ni^{2+} ion migration from the transition-metal slab to the Li slab during charge–discharge processes *via* stabilization of the valence of the Ni ions or the generation of electrostatic repulsion.

To further improve the electrochemical performance of Ni-rich layered materials, precursors using different doping element sites have been designed, and the effects on the final products have been investigated. For example, Ni-rich layered $LiNi_{1-x-y}Co_xMn_yO_2$ materials with novel structures, such as core–shell,[11–13] concentration-gradient,[14–16] and full concentration-gradient[17–19] structures, have been designed and synthesized by different research groups. Through structure design, the electrochemical performance and safety have been further enhanced. However, it remains controversial whether the core–shell and concentration-gradient structures of the precursors can be maintained in the final products. Some researchers have reported that the diffusion of the cations between the core and shell phases occurs during sintering, which makes *a priori* design of a particular core–shell structure difficult.[20–24] However, Li–Ni–Co–Mn–O_2 materials synthesized from precursors with core–shell, concentration-gradient, or full concentration-gradient structures still exhibit improved electrochemical performance. In our recent work,[25] three types of $LiNi_{0.88}Co_{0.12}O_2$ materials were synthesized from three different structured precursors, namely completely coated $0.88Ni(OH)_2@0.12Co(OH)_2$, semi-coated and semi-doped $0.94Ni_{0.936}Co_{0.064}(OH)_2@0.06Co(OH)_2$, and completely doped $Ni_{0.88}Co_{0.12}(OH)_2$. Although the core–shell structures of the completely coated and semi-coated/semi-doped precursors disappeared after sintering with $LiOH\cdot H_2O$ and the three

[a]State Key Laboratory of Chemical Resource Engineering, Beijing University of Chemical Technology, Beijing 100029, China. E-mail: yangws@mail.buct.edu.cn
[b]Sinopec Research Institute of Petroleum Processing, Beijing 100083, China

† Electronic supplementary information (ESI) available. See DOI: 10.1039/c8ra10116g

products maintained the same structures, the product synthesized from the completely coated $0.88Ni(OH)_2@0.12Co(OH)_2$ precursor still exhibited the best electrochemical performance.

Therefore, it is of interest to determine the changing regularity of precursor structures during the sintering reaction process and its effect on the electrochemical performance of the final materials. In this work, a series of experiments were conducted to investigate the effects of the Co site and content on the electrochemical performance of two types of $LiNi_{1-x}Co_xO_2$ materials derived from coated $(1-x)Ni(OH)_2@xCo(OH)_2$ and doped $Ni_{1-x}Co_x(OH)_2$ precursors ($x = 0.04$, 0.08, 0.12, 0.16). In addition, the changing trends of the difference as a function of the Co content were also investigated. The Co site and content in the precursor were observed to affect the electrochemical properties of the material, with the material synthesized from the coated precursor exhibiting improved electrochemical properties and the difference between the electrochemical properties of the two materials decreasing with increasing Co content.

2. Experimental

2.1. Material synthesis

2.1.1. Synthesis of precursors with coated structures. The coated $(1-x)Ni(OH)_2@xCo(OH)_2$ precursors ($x = 0.04$, 0.08, 0.12, 0.16) were synthesized using a co-precipitation method. An aqueous solution of 2.0 M $NiSO_4 \cdot 6H_2O$ was pumped into a continuously stirred tank reactor (CSTR, capacity = 50 L). At the same time, a NaOH solution of 6.0 M and a desired amount of NH_4OH solution as the chelating agent were separately fed into the reactor. The concentration of the solution, pH, temperature, and stirring speed of the mixture in the reactor were carefully controlled. The resulting spherical $Ni(OH)_2$ was continuously reacted with different amounts of $CoSO_4 \cdot 7H_2O$ to synthesize the $(1-x)Ni(OH)_2@xCo(OH)_2$ ($x = 0.04$, 0.08, 0.12, 0.16) precursors. The precursors were filtered and washed with deionized water several times and then dried at 120 °C for 15 h.

2.1.2. Synthesis of precursors with doped structures. The doped $Ni_{1-x}Co_x(OH)_2$ precursors ($x = 0.04$, 0.08, 0.12, 0.16) were also synthesized using a co-precipitation method. An aqueous solution containing $NiSO_4 \cdot 6H_2O$ and $CoSO_4 \cdot 7H_2O$ [Ni : Co = $(1-x)$: x mole ratio] with a concentration of 2.0 M was pumped into a CSTR (capacity = 50 L). At the same time, a 6.0 M NaOH solution and a desired amount of NH_4OH solution as the chelating agent were separately fed into the reactor. The concentration of the solution, pH, temperature, and stirring speed of the mixture in the reactor were carefully controlled. The precursors were filtered and washed with deionized water several times and then dried at 120 °C for 15 h.

2.1.3. Synthesis of $LiNi_{1-x}Co_xO_2$ materials. To synthesize the $LiNi_{1-x}Co_xO_2$ materials, the precursors were mixed with $LiOH \cdot H_2O$ [Li : (Ni + Co) = 1.05 : 1 mole ratio] and thoroughly ball-milled for 3 h. The mixtures were preheated at 580 °C for 5 h, and the calcined materials were then ball-milled for 1 h to obtain the intermediate products. For $x = 0.04$–0.12, the second stage of the synthesis was performed at 680 °C for 20 h in a flowing O_2 atmosphere of 1 L min^{-1}. For $x = 0.16$, the synthesis temperature was 720 °C. Then, the final $LiNi_{1-x}Co_xO_2$ materials derived from the different structured precursors were obtained.

2.2. Material characterization

The compositions of the as-prepared precursors and lithium oxides were determined using inductively coupled plasma atomic emission spectrometry (ICP-AES; SPS-7800, Japan). The particle morphologies of the as-prepared precursors and lithium oxides were examined using scanning electron microscopy (SEM; Supra 55, ZEISS, Germany). Powder X-ray diffraction (XRD, Ultima III, Rigaku, Japan) measurements using Cu K_α radiation ($\lambda = 0.154$ nm) were employed to identify the crystalline phases of the synthesized materials. XRD data were obtained in the 2θ range of 10–80° at a scan rate of 5° min^{-1}. The lattice parameters were calculated from the XRD data using the least-squares method.

2.3. Electrochemical measurements

The electrochemical performance of each synthesized powder was assessed using a 2032 coin-type cell. The cell consisted of a cathode and a lithium metal anode separated by a porous polypropylene film. The cathode was fabricated using a mixture of the prepared powder (80 wt%), carbon black (10 wt%), and polyvinylidene fluoride (10 wt%) in *N*-methyl-2-pyrrolidinone. The slurry was spread onto Al foil and dried in a vacuum oven at 110 °C. The electrolyte used was 1 M $LiPF_6$ in EC–DMC–DEC (1 : 1 : 1 volume ratio). The cells were charged and discharged by applying a constant current density of 20 mA g^{-1} (0.1C) for the initial 4 cycles and then cycled at 40 mA g^{-1} (0.2C) for the subsequent 96 cycles in the voltage range of 2.75–4.3 V at room temperature on a LAND CT-2001A test system (Wuhan).

3. Results and discussion

3.1. Chemical composition

ICP-AES analysis was performed on the two different structural precursors as well as on the final products synthesized from these precursors, and the results are presented in Table 1. Although the synthesis processes of the materials differed, the Ni and Co contents in the precursors and final products were basically the same as the feed ratios.

3.2. SEM characterization

Because of the different synthesis processes used to prepare the precursors, their morphologies differed. SEM images of the coated $(1-x)Ni(OH)_2@xCo(OH)_2$ precursors are presented in Fig. 1(a–d). The same $Ni(OH)_2$ powders were used to synthesize four coated precursors with different Co contents. The particle morphology of $Ni(OH)_2$ was spherical, and the average particle diameter was approximately 10 μm. In our previous work,[25] atomic emission spectroscopy (AES) was used to determine the radial concentration distribution of Ni and Co in a $0.88Ni(OH)_2@0.12Co(OH)_2$ precursor, revealing that the surface of $Ni(OH)_2$ was coated with a $Co(OH)_2$ layer, forming a core–shell structure. Furthermore, as clearly observed in

Table 1 Chemical compositions of two different structural precursors and final products synthesized from these precursors determined using ICP-AES analysis

Ni/Co feed ratio	Composition of precursor		Composition of final product	
	Coated precursor	Doped precursor	From coated precursor	From doped precursor
96/4	$0.959Ni(OH)_2@0.041Co(OH)_2$	$Ni_{0.958}Co_{0.042}(OH)_2$	$Li_{1.036}Ni_{0.959}Co_{0.041}O_2$	$Li_{1.039}Ni_{0.958}Co_{0.042}O_2$
92/8	$0.919Ni(OH)_2@0.081Co(OH)_2$	$Ni_{0.919}Co_{0.081}(OH)_2$	$Li_{1.036}Ni_{0.919}Co_{0.081}O_2$	$Li_{1.038}Ni_{0.919}Co_{0.081}O_2$
88/12	$0.877Ni(OH)_2@0.123Co(OH)_2$	$Ni_{0.876}Co_{0.124}(OH)_2$	$Li_{1.038}Ni_{0.877}Co_{0.123}O_2$	$Li_{1.037}Ni_{0.876}Co_{0.124}O_2$
84/16	$0.834Ni(OH)_2@0.166Co(OH)_2$	$Ni_{0.843}Co_{0.157}(OH)_2$	$Li_{1.037}Ni_{0.834}Co_{0.166}O_2$	$Li_{1.035}Ni_{0.843}Co_{0.157}O_2$

Fig. 1(a–c), the smoothness of the surface of the material decreased with increasing Co content, and almost no $Co(OH)_2$ particles were observed in the single phase. This finding indicates that when the $Co(OH)_2$ coating amount was relatively low ($x \leq 0.12$), most of the $Co(OH)_2$ material was coated on the surface of the $Ni(OH)_2$ particles. However, when the coating amount x was increased to 0.16, as shown in Fig. 1(d), some $Co(OH)_2$ particles with small particle size were not coated on the surface of $Ni(OH)_2$ particles and instead existed in a single phase. This result indicates that the amount of the coating layer is limited and that the coating amount cannot be increased without restriction. As observed in Fig. 1(e–h), unlike the coated precursors, there was little difference in the morphologies of the four doped $Ni_{1-x}Co_x(OH)_2$ precursors with varying x in the range of 0.04–0.16. The morphologies of all four doped precursors were spherical or spherical-like with an average particle size of approximately 10 μm. This result was expected because $Ni(OH)_2$ and $Co(OH)_2$ possess similar structures and can be composited in any proportion.

Fig. 2 presents SEM images of the final $LiNi_{1-x}Co_xO_2$ oxides. The spherical morphologies of the precursors were maintained even after high-temperature calcination. Additionally, no obvious differences were observed among the morphologies of the final $LiNi_{1-x}Co_xO_2$ materials (x = 0.04, 0.08, 0.12, 0.16) regardless of whether the precursor had a coated or doped structure. For the $LiNi_{1-x}Co_xO_2$ materials synthesized from the coated precursors, Ni and Co metal ions diffused into each other, and the core–shell structure disappeared during the high-temperature calcination,[24,25] resulting in the same structure and radial elemental distribution as those of the lithium oxides synthesized from the doped precursors.

3.3. Crystal structure

The $LiNi_{1-x}Co_xO_2$ materials were synthesized by lithiating the different structured hydroxide precursors with $LiOH \cdot H_2O$ using a two-step high-temperature heat-treatment process. The intermediate products after the first stage of calcination and the final products were characterized using XRD. XRD patterns of the intermediate products derived from the coated precursors are presented in Fig. 3. The clear (003) and (104) reflection peaks corresponding to $LiNiO_2$ oxides after calcination at 580 °C for 5 h indicate the basic α-$NaFeO_2$ layered structure of the intermediate products. However, splitting of the (006)/(012) and (018)/(110) peaks did not occur, indicating that a well-ordered layered structure was not completely developed. Additionally, for x = 0.04 and 0.08, no peaks corresponding to the $Li_{1-x}CoO_2$ phase appeared in the XRD patterns (Fig. 3(a) and (b)). This finding may be attributed to the small amount and weak peak intensity of $Li_{1-x}CoO_2$ materials; for $x \geq 0.12$, impurity peaks corresponding to the $Li_{1-x}CoO_2$ phase appeared in the XRD patterns (Fig. 3(c–d)). The above results indicate that at 580 °C,

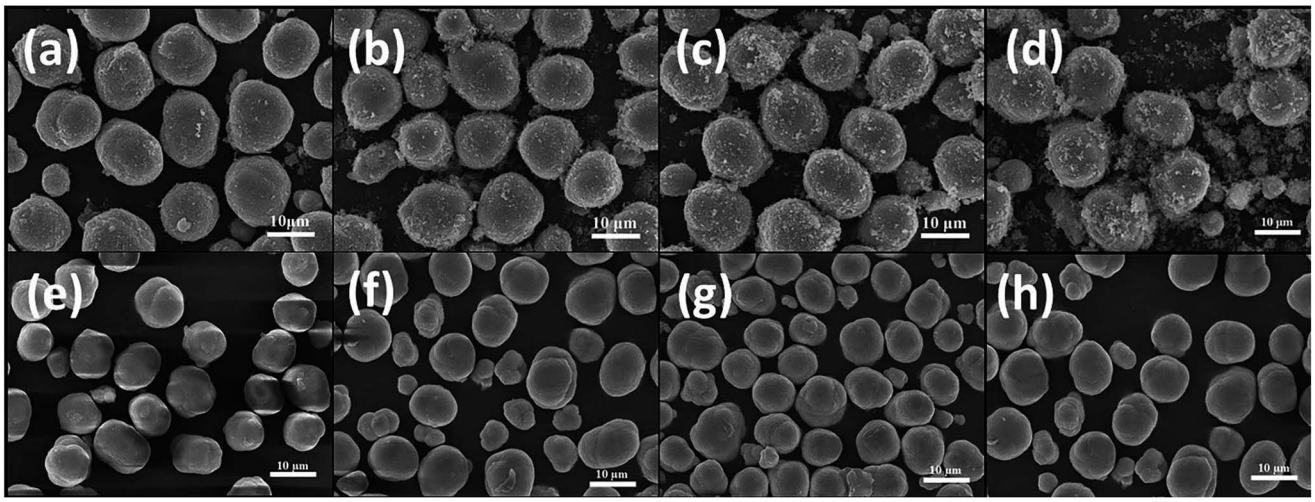

Fig. 1 SEM images of coated $(1-x)Ni(OH)_2@xCo(OH)_2$ precursors, x = (a) 0.04, (b) 0.08, (c) 0.12, and (d) 0.16, and doped $Ni_{1-x}Co_x(OH)_2$ precursors, x = (e) 0.04, (f) 0.08, (g) 0.12, and (h) 0.16.

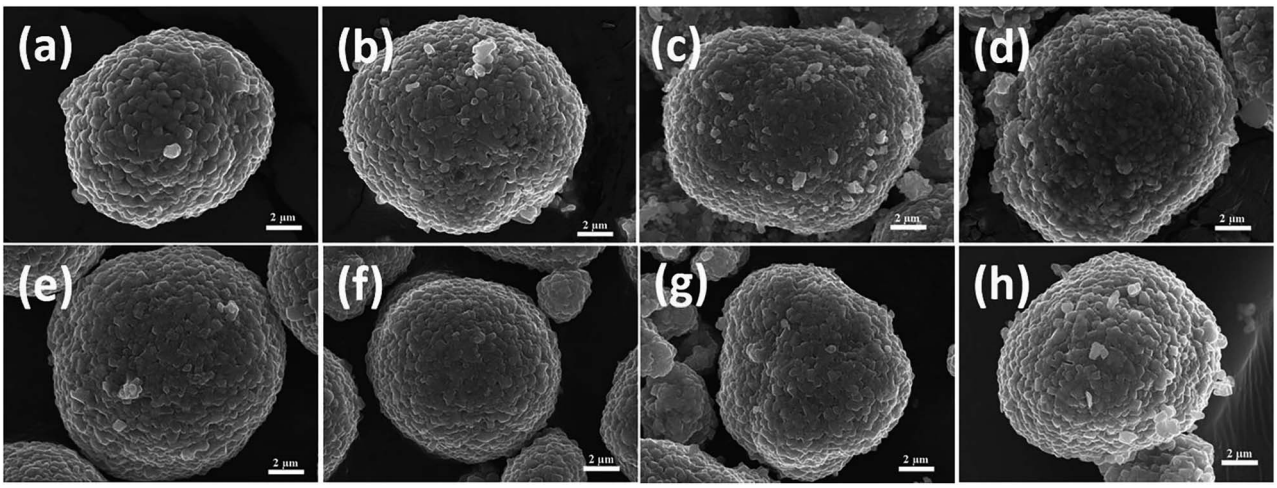

Fig. 2 SEM images of $LiNi_{1-x}Co_xO_2$ materials synthesized from coated precursors, x = (a) 0.04, (b) 0.08, (c) 0.12, and (d) 0.16, and $LiNi_{1-x}Co_xO_2$ materials synthesized from doped precursors, x = (e) 0.04, (f) 0.08, (g) 0.12, and (h) 0.16.

the interdiffusion degree between Ni and Co metal ions was very small and the intermediate products were core–shell-structured $(1-x)LiNiO_2@xLiCoO_2$ materials. The XRD patterns of the four intermediate products derived from the doped $Ni_{1-x}Co_x(OH)_2$ precursors were similar (Fig. 4): (003) and (104) peaks appeared, and splitting of the (006)/(012) and (018)/(110) peaks was not observed. No impurity peaks appeared in the XRD patterns, indicating that the intermediate product obtained from the doped precursor after the first stage of calcination did not contain the $Li_{1-x}CoO_2$ phase with increasing Co content.

Fig. 5 presents the XRD patterns of the final $LiNi_{1-x}Co_xO_2$ (x = 0.04, 0.08, 0.12, 0.16) products synthesized from the coated $(1-x)Ni(OH)_2@xCo(OH)_2$ and doped $Ni_{1-x}Co_x(OH)_2$ precursors. All the diffraction peaks can be indexed to hexagonal $LiNiO_2$ with a well-ordered layered structure (JCPDS no. 09-0063), indicating the high phase purity. Unlike the intermediate products for the coated precursors, the peaks corresponding to the $Li_{1-x}CoO_2$ coating in the final product completely disappeared because the Ni and Co metal ions completely diffused into each other, forming a homogeneous structure.

The structural parameters of the as-prepared samples were calculated using the least-squares method, and the results are summarized in Table 2. With increasing Co content x from 0.04 to 0.16, the lattice parameters c and a and cell volume decreased because the smaller-sized Co^{3+} replaced Ni^{2+}, resulting in crystal volume shrinkage. The c/a ratios of the final products were both larger than 4.9, further confirming the highly layered structure and lower cation mixing for both samples.[26] In addition, the intensity ratio $I_{(003)}/I_{(104)}$ increased upon increasing x from 0.04 to 0.12 for the two types of final $LiNi_{1-x}Co_xO_2$ products, indicating that higher Co content led to a lower degree of Li^+/Ni^{2+} cation mixing and a better layered structure. In addition, the $I_{(003)}/I_{(104)}$ intensity ratios of the $LiNi_{1-x}Co_xO_2$ products synthesized from the coated precursor were higher than those of the products synthesized from the doped precursor for the same Co content x. The coating of $Co(OH)_2$ on the surface of spherical $Ni(OH)_2$ particles can have a "barrier effect", decreasing the rate of Li diffusing into the core NiO material

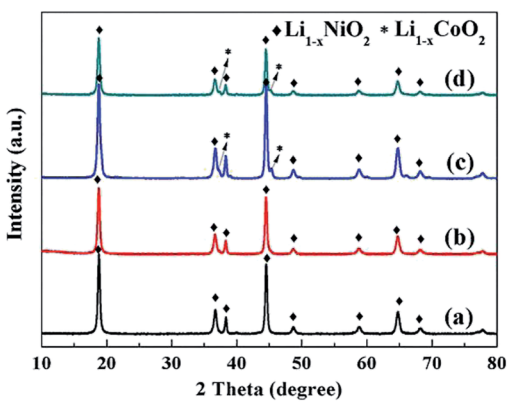

Fig. 3 XRD patterns of intermediate $LiNi_{1-x}Co_xO_2$ products synthesized from coated precursors after being calcined at 580 °C for 5 h: x = (a) 0.04, (b) 0.08, (c) 0.12, and (d) 0.16.

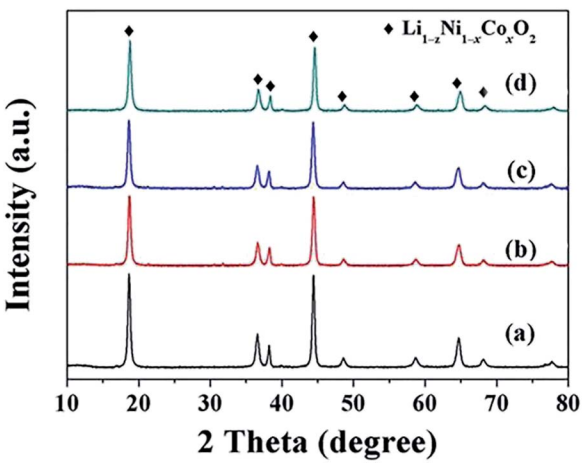

Fig. 4 XRD patterns of intermediate $LiNi_{1-x}Co_xO_2$ products synthesized from doped precursors after being calcined at 580 °C for 5 h: x = (a) 0.04, (b) 0.08, (c) 0.12, and (d) 0.16.

Table 2 Lattice parameters and $I_{(003)}/I_{(104)}$ values as a function of x in $LiNi_{1-x}Co_xO_2$ materials

	From coated $(1-x)Ni(OH)_2@xCo(OH)_2$				From doped $Ni_{1-x}Co_x(OH)_2$			
Items	$x = 0.04$	$x = 0.08$	$x = 0.12$	$x = 0.16$	$x = 0.04$	$x = 0.08$	$x = 0.12$	$x = 0.16$
c (Å)	14.218	14.194	14.153	14.127	14.226	14.210	14.145	14.140
a (Å)	2.881	2.875	2.865	2.855	2.885	2.880	2.861	2.856
c/a	4.935	4.937	4.940	4.948	4.931	4.934	4.944	4.951
Volume (Å^3)	102.20	101.60	100.60	99.72	102.54	102.07	100.27	99.88
$I_{(003)}/I_{(104)}$	1.504	1.682	1.865	1.803	1.435	1.437	1.503	1.870

and leaving sufficient time for the oxidation of Ni^{2+} ions to Ni^{3+} ions as much as possible, thus resulting in a decrease of the Li^+/Ni^{2+} cation mixing and leading to a better layered structure.[25] However, the $I_{(003)}/I_{(104)}$ intensity ratio of the $LiNi_{0.84}Co_{0.16}O_2$ material synthesized from the coated $0.84Ni(OH)_2@0.16Co(OH)_2$ precursor was smaller than that of the $LiNi_{0.84}Co_{0.16}O_2$ material synthesized from the doped $Ni_{0.84}Co_{0.16}(OH)_2$ precursor and even smaller than that of the $LiNi_{0.88}Co_{0.12}O_2$ synthesized from the coated $0.88Ni(OH)_2@0.12Co(OH)_2$ precursor. Most likely, some $Co(OH)_2$ particles precipitated in a single phase during the synthesis of the $0.84Ni(OH)_2@0.16Co(OH)_2$ coated precursor, resulting in a composite of $LiNi_{1-x}Co_xO_2$ ($x < 0.16$) and a very small amount of $LiCoO_2$ as the final product. The optimal temperature (720 °C) of Ni-rich material is not suitable for the formation of $LiCoO_2$; therefore, the layered structure of the final $LiNi_{0.84}Co_{0.16}O_2$ material was inferior to that of the $LiNi_{0.88}Co_{0.12}O_2$ material.

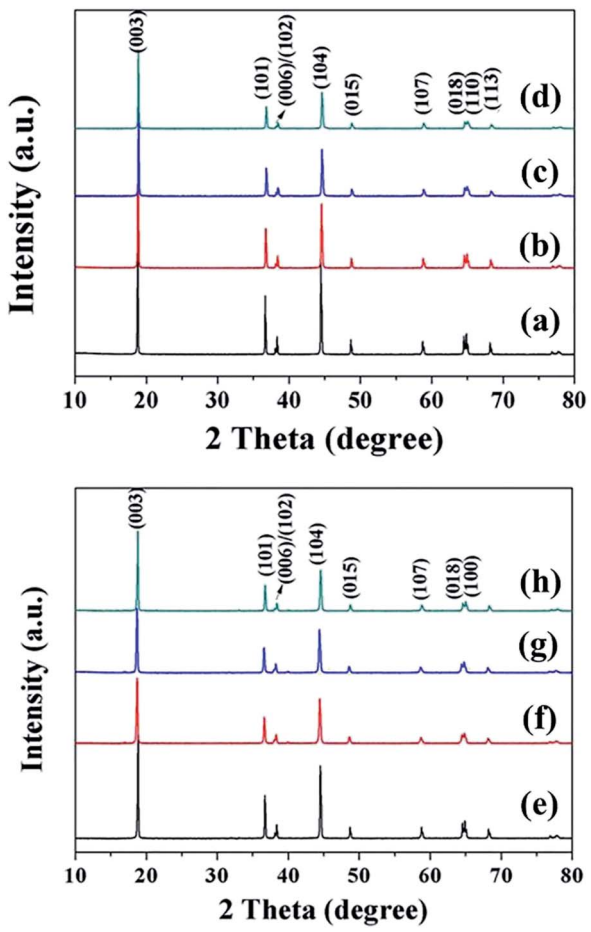

Fig. 5 XRD patterns of final $LiNi_{1-x}Co_xO_2$ products synthesized from coated $(1-x)Ni(OH)_2@xCo(OH)_2$ precursors, x = (a) 0.04, (b) 0.08, (c) 0.12, and (d) 0.16, and doped $Ni_{1-x}Co_x(OH)_2$ precursors, x = (e) 0.04, (f) 0.08, (g) 0.12, and (h) 0.16.

3.4. Electrochemical performance

We investigated the differences in the electrochemical performance of $LiNi_{1-x}Co_xO_2$ materials derived from the different structured precursors as a function of the Co content x. Coin-type cells using $LiNi_{1-x}Co_xO_2$ as the positive electrode and Li metal as the negative electrode were used for the electrochemical measurements. The cells were charged and discharged at a constant current density of 20 mA g^{-1} for the initial four cycles and 40 mA g^{-1} for the subsequent 96 cycles. The initial charge–discharge curves and the cycling performance are shown in Fig. 6. As observed in Fig. 6(a), the $LiNi_{1-x}Co_xO_2$ materials derived from the coated precursors exhibited discharge specific capacities of 210.2, 217.5, 213.8, and 205.3 mA h g^{-1} for $x = 0.04$, 0.08, 0.12, and 0.16, respectively. These results indicate that the highest discharge specific capacity was obtained for the $LiNi_{0.92}Co_{0.08}O_2$ material and not $LiNi_{0.96}Co_{0.04}O_2$ with the highest Ni content. As observed in Fig. 6(b), the $LiNi_{1-x}Co_xO_2$ materials derived from the doped precursors exhibited discharge specific capacities of 203.3, 212.8, 210.2, and 202.7 mA h g^{-1} for $x = 0.04$, 0.08, 0.12, and 0.16, respectively. The highest discharge specific capacity was also obtained for the $LiNi_{0.92}Co_{0.08}O_2$ material. The $Li/LiNi_{0.96}Co_{0.04}O_2$ cells prepared using the two different structured precursors exhibited initial coulombic efficiencies of approximately 88%, whereas the $Li/LiNi_{1-x}Co_xO_2$ ($x = 0.08$, 0.12, 0.16) cells prepared from the two different structured precursors exhibited similar initial coulombic efficiencies of approximately 91–93% at 0.1C. Therefore, it is reasonable to conclude that the $LiNi_{0.96}Co_{0.04}O_2$ materials with such high Ni content had a poor layered structure, which resulted in a high irreversible capacity and lower initial discharge capacity. The 100th capacity retention ratios of the $LiNi_{1-x}Co_xO_2$ materials synthesized from the coated precursors (Fig. 6(c)) were 60.7%, 75.4%, 88.5%, and 86.6% for $x = 0.04$, 0.08, 0.12, and 0.16, respectively. The best cycling performance was achieved for the $LiNi_{0.88}Co_{0.12}O_2$ material. In comparison, for the $LiNi_{1-x}Co_xO_2$ materials synthesized from the doped precursors (Fig. 6(d)), the capacity

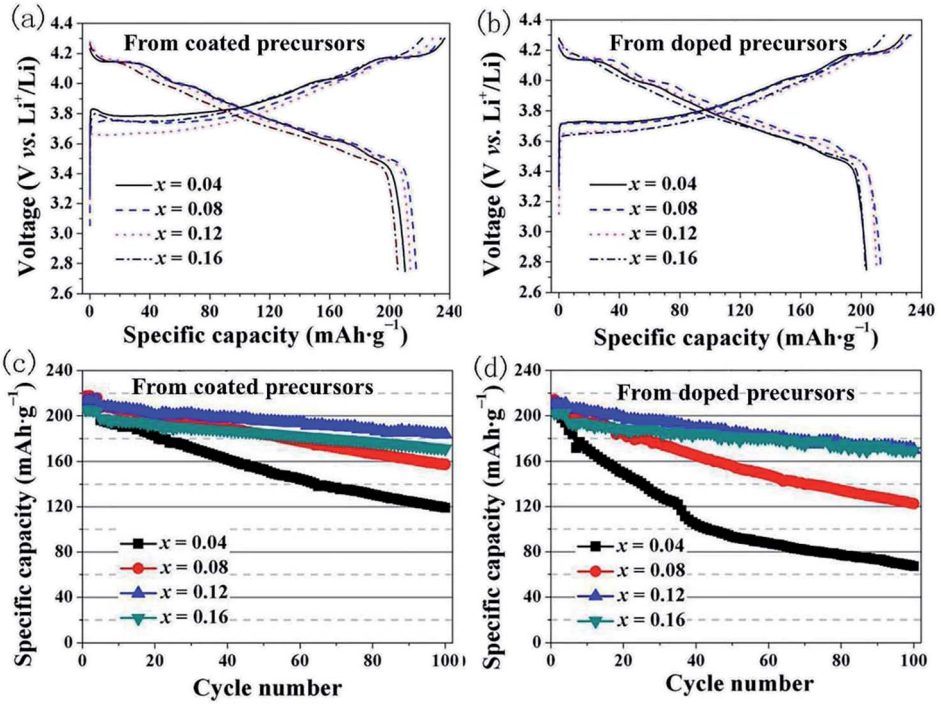

Fig. 6 Initial charge–discharge curves for product prepared from: (a) coated precursors and (b) doped precursors; cycling performance of $LiNi_{1-x}Co_xO_2$ (x = 0.04, 0.08, 0.12, 0.16) materials synthesized from (c) coated precursors and (d) doped precursors.

retention ratios after 100 cycles were 36.0%, 60.6%, 82.6%, and 87.1%, respectively, and the cycling performance increased with increasing Co content, similar to results previously reported in the literature.[20] The rate performances of the materials at different current rates indicate that the $LiNi_{0.88}Co_{0.12}O_2$ material prepared from the coated precursor exhibited the optimal performance, as shown in Fig. S1.†

To further compare the different effects of Co in the $LiNi_{1-x}Co_xO_2$ products prepared from the coated and doped precursors with the same Co content, the results of the initial discharge specific capacity and 100-cycle capacity retention ratios as a function of the Co content x are summarized in Fig. 7. Δ_{Ca} is the difference in the initial discharge specific capacity of the $LiNi_{1-x}Co_xO_2$ products prepared from the two different structural precursors, and Δ_{Ret} is the difference in the capacity retention after 100 cycles. With increasing Co content x, the specific capacity and 100-cycle capacity retention ratio of the two types of materials showed the same tendencies. Moreover, the initial discharge specific capacities of the products prepared from the coated precursors were still higher than those prepared from the doped precursors with the same Co content x, as observed in Fig. 7(a); however, Δ_{Ca} decreased with increasing Co content x. The capacity retention ratios of the two types of materials were similar, as observed in Fig. 7(b), except that the $LiNi_{1-x}Co_xO_2$ product derived from the doped precursor exhibited a slightly higher capacity retention ratio at a Co content of x = 0.16. The electrochemical performance of the $LiNi_{1-x}Co_xO_2$ product prepared from the coated precursor was generally superior to that of the product prepared from the doped precursor. This finding can be attributed to the "barrier effect" of the coated $Co(OH)_2$ layer, which left sufficient time for the oxidation of Ni^{2+} ions to Ni^{3+} as much as possible and thus decreased the Li^+/Ni^{2+} cation mixing and led to the high electrochemical performance. The cycling performance of the $LiNi_{0.84}Co_{0.16}O_2$ synthesized from the doped precursor exceeded that of the material synthesized from the coated precursor

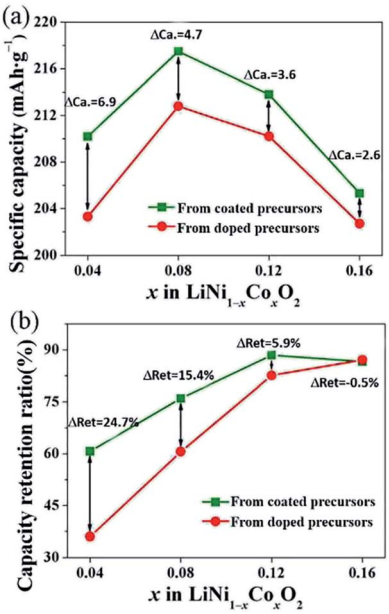

Fig. 7 Initial discharge specific capacity and 100th capacity retention of $LiNi_{1-x}Co_xO_2$ materials synthesized from different structured precursors as a function of Co content x.

because of the high coating content: some $Co(OH)_2$ materials could not be coated on the surface of the $Ni(OH)_2$ particles and formed in a single phase; thus, they did not have a coating effect. The $Co(OH)_2$ existing in the single phase could not be transformed into $LiCoO_2$ materials with good electrochemical performance under synthesis conditions suitable for Ni-rich materials.

In summary, the products prepared from the coated precursors were generally superior to the products prepared from the doped precursors for the preparation of $LiNi_{1-x}Co_xO_2$ materials, especially at lower Co contents. However, because there is an upper limit to the effective coating layer amount, for high coating amounts, such as Co content $x = 0.16$, the difference in the electrochemical properties of the products prepared from the coated and doped precursors was reduced. The electrochemical properties of the products prepared from the coated precursor were sometimes even worse than those of the products prepared from the doped precursor at higher Co content.

4. Conclusions

$LiNi_{1-x}Co_xO_2$ materials were successfully synthesized from coated $(1-x)Ni(OH)_2@xCo(OH)_2$ and doped $Ni_{1-x}Co_x(OH)_2$ precursors. The differences in the electrochemical performances of the $LiNi_{1-x}Co_xO_2$ materials derived from the different structured precursors and the changing trends of the difference as a function of the Co content x were investigated. For $x \leq 0.12$, the $LiNi_{1-x}Co_xO_2$ materials synthesized from the coated precursors exhibited more stable structures and better electrochemical performance. The $LiNi_{0.88}Co_{0.12}O_2$ material prepared from the coated precursor exhibited a high discharge specific capacity of 213.8 mA h g^{-1} at 0.1C and good cycling performance with a capacity retention of 88.5% after 100 cycles at 0.2C. In contrast, for $x > 0.12$, the $LiNi_{1-x}Co_xO_2$ materials synthesized from the doped precursor were preferred because some $Co(OH)_2$ could not be coated on the surface of the core materials, resulting in poorer electrochemical performance of the final $LiNi_{1-x}Co_xO_2$ products.

Conflicts of interest

There are no conflicts to declare.

Acknowledgements

This work was funded by the National Natural Science Foundation of China (U1407118 and 21521005), and Research Institute of Petroleum Processing Sinopec (218025-1).

References

1 F. Schipper, M. Dixit, D. Kovacheva, M. Talianker, O. Haik, J. Grinblat, E. M. Erickson, C. Ghanty, D. T. Major, B. Markovsky and D. Aurbach, *J. Mater. Chem. A*, 2016, **4**, 16073–16084.
2 H. Xie, K. Du, G. Hu, Z. Peng and Y. Cao, *J. Phys. Chem. C*, 2016, **120**, 3235–3241.
3 B. Huang, X. Li, Z. Wang, H. Guo, L. Shen and J. Wang, *J. Power Sources*, 2014, **252**, 200–207.
4 M. Ko, S. Chae, J. Ma, N. Kim, H. W. Lee, Y. Cui and J. Cho, *Nat. Energy*, 2016, **1**, 16113.
5 P. Zhou, H. Meng, Z. Zhang, C. C. Chen, Y. Lu, J. Cao, F. Cheng and J. Chen, *J. Mater. Chem. A*, 2017, **5**, 12361.
6 Y. Zhang, M. Nie and Z. Wang, *RSC Adv.*, 2016, **6**, 65941.
7 S. U. Woo, B. C. Park, C. S. Yoon, S. T. Myung, J. Prakash and Y. K. Sun, *J. Electrochem. Soc.*, 2007, **154**, A649.
8 P. Oh, S.-M. Oh, W. Li, S. Myeong, J. Cho and A. Manthiram, *Adv. Sci.*, 2016, **3**, 11.
9 Z. Zhang, D. Chen and C. Chang, *RSC Adv.*, 2017, **7**, 51721.
10 G. Wang, L. Yi and X. Wang, *RSC Adv.*, 2016, **6**, 46325.
11 Y. K. Sun, S. Myung, A. Byungchun Park and K. Amine, *Chem. Mater.*, 2006, **18**, 5159–5163.
12 Y. K. Sun, S. Myung, K. I. M. Myung-Hoon and K. I. M. Jung-Hyun, *Electrochem. Solid-State Lett.*, 2006, **9**, A171–A174.
13 Y. K. Sun, S. T. Myung, M. H. Kim, J. Prakash and K. Amine, *J. Am. Chem. Soc.*, 2005, **127**, 13411–13418.
14 Y. K. Sun, B.-R. Lee, H.-J. Noh, H. Wu, S.-T. Myung and K. Amine, *J. Mater. Chem.*, 2011, **21**, 10108.
15 Y. K. Sun, D.-H. Kim, C. S. Yoon, S.-T. Myung, J. Prakash and K. Amine, *Adv. Funct. Mater.*, 2010, **20**, 485–491.
16 J. Wang, C. Du, C. Yan, X. Xu and Y. Gao, *RSC Adv.*, 2016, **6**, 26307.
17 Y. K. Sun, Z. Chen, H. J. Noh, D. J. Lee, H. G. Jung, Y. Ren, S. Wang, S. Y. Chong, S. T. Myung and K. Amine, *Nat. Mater.*, 2012, **11**, 942–947.
18 U. H. Kim, E.-J. Lee, C. S. Yoon, S.-T. Myung and Y.-K. Sun, *Adv. Energy Mater.*, 2016, **6**, 1601417.
19 Z. Sun, D. Wang, Y. Fan and L. Niu, *RSC Adv.*, 2016, **6**, 103747.
20 J. Li, R. Doig, H. Liu, G. Botton and J. R. Dahn, *J. Electrochem. Soc.*, 2016, **163**, A2841–A2848.
21 X. Yang, X. Wang, L. Hu, G. Zou, S. Su, Y. Bai, H. Shu, Q. Wei, B. Hu, L. Ge, D. Wang and L. Liu, *J. Power Sources*, 2013, **242**, 589–596.
22 J. Li, R. Shunmugasundaram, R. Doig and J. R. Dahn, *Chem. Mater.*, 2016, **28**, 162–171.
23 Y. Zhang, H. Shi, D. Song, H. Zhang, X. Shi and L. Zhang, *J. Power Sources*, 2016, **327**, 38–43.
24 J. Li, R. Doig, J. Camardese, K. Plucknett and J. R. Dahn, *Chem. Mater.*, 2015, **27**, 7765–7773.
25 G. Li, L. Qi, P. Xiao, Y. Yu, X. Chen and W. Yang, *Electrochim. Acta*, 2018, **270**, 319–329.
26 L. Zhang, J. Wang and X. Yang, *ACS Appl. Mater. Interfaces*, 2018, **10**, 11663–11670.